



Transactions of the **13th International Conference on Structural Mechanics in Reactor Technology (SMiRT 13)**, Escola de Engenharia - Universidade Federal do Rio Grande do Sul, Porto Alegre, Brazil, August 13-18, 1995

A boundary element and optimization approach for the ill-posed inverse problem of contact stress reconstruction

Bezerra, L.M.

CNEN/SP-IPEN -Comissão Nacional de Energia Nuclear, São Paulo, SP, Brazil

1 INTRODUCTION

In solid mechanics, the problem of Contact Stress Reconstruction (CSR), based on measurements from sensors located on the boundary or at interior points of the body, constitutes an IPP. This type of problem can be found, for example, in characterizing tractions at inaccessible regions of critical components in sensitive mechanical equipment, or characterizing tractions on a portion of the body embedded in a hazardous environment. Another application is the determination of tractions in a physical truncation. Such tractions may be needed in a partial mesh discretization of the body. In these cases, the internal data are generally not only more accurate, but easier to assess. Techniques like strain gages, photoelasticity, coating, and speckle interferometry, among others, are reliable experimental methods for the determination of deformation, strain and stress tensors at the boundary of or inside a body (Weathers et al. 1985).

Schnur and Zabarás (1990) presented the boundary condition reconstruction for elastostatics application using the FEM in conjunction with spatial regularization. In this paper, optimization approach was not employed and only magnitudes of simple traction distributions at a fix location on the surface of the body were determined.

In this paper, the IPP of CSR is formulated as a constrained nonlinear optimization problem in a BEM framework. Using function specifications for the unknown contact stresses, the solution procedure adopted seeks to minimize the difference between the experimental data and the corresponding computed quantities. Geometric constrains forcing the solution to lies within a specific portion of the boundary of the body are also imposed. The design sensitivities required in the optimization procedure are obtained by the implicit differentiation (Saigal et al. 1989) of the BEM integral equations. Examples involving the determination of the magnitude, extent, and location of contact stresses are presented in this paper. Finally, it is important to notice that computational techniques for the solution of the IPP of CSR may provide an evaluation tool for identifying contact regions in neighboring objects, as well as hybrid experimental and numerical methods for the analyses of solids (Weathers et al. 1985, Balas et al. 1983).

2 DEFINITION OF THE PROBLEM

Consider that in Fig.1 the external boundary Γ of the solid Ω got in touch with another body, and the contact traction Φ has its magnitude, extent, and location unknown.

The reconstruction of Φ , along Γ and based on internal or external experimental data in terms of displacements, stresses, or strains constitutes an IPP. In mathematical notation, this can be expressed as

$$\begin{aligned} \sigma_{ij}(x) &= -b_j(x); \quad \forall x \in \Omega & (1) \\ \sigma_{ij}(x) &= \lambda \delta_{ij} \epsilon_{kk}(x) + 2\mu \epsilon_{ij}(x); \quad \forall x \in \Omega & (2) \\ \epsilon_{ij}(x) &= \frac{1}{2} [u_{ij}(x) + u_{ji}(x)]; \quad \forall x \in \Omega & (3) \\ \sigma_{ij}(y) n_i(y) &= \bar{t}_i; \quad y \in \Gamma_1 & (4) \\ u_i(y) &= \bar{u}_i; \quad y \in \Gamma_2, \text{ and} & (5) \\ \phi_k &= \phi_i(x_k); \quad x_k \in \Gamma^*, \text{ or } x_k \in \Gamma & (6) \end{aligned}$$

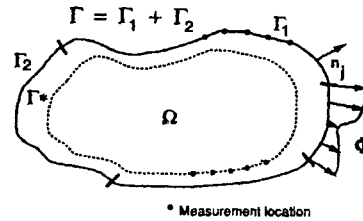


Fig.1-Unknown boundary traction

where x and y are position vectors. $\sigma_{ij}, \epsilon_{ij}, b_j, u_i, t_i$, are; stress, strain, body force, displacement, and traction, respectively. \bar{t}_i and \bar{u}_i are prescribed tractions and displacements, respectively. λ and μ are the Lamé's constants. δ_{ij} is the Kronecker's delta. $\hat{\phi}_{ik}$ with $(i = x, y)$ and $(k = 1, 2, 3 \dots m)$ are simulated experimental quantities along the direction " i " and at location " k ," $\hat{\phi}_{ik}$ may be internal or external data in terms of displacements, stresses, or strains. $\hat{\phi}_{ik}$ is simulated from the solution obtained from a boundary element analysis with the actual contact stress applied.

To solve the IPP of CSR the best-fit method using optimization technique is used. A residual function - difference between the model prediction and the measured data - is minimized. The residual function $f(z)$ is the difference between $\hat{\phi}_{ik}$ and the corresponding computed quantities ϕ_{ik} multiplied by a weighting parameter " w_{ik} " to enhance numerical sensitivity. $\{\hat{\phi}\}$ is the data vector, and the mapping $Az = \{\hat{\phi}\}$ corresponds to the computed quantity. $\{\phi\}$ is obtained in terms of the design variables which specify magnitude, extent, and location of the contact stress. The objective function to minimize is

$$f(z) = w \sum_{k=1}^m \sum_{i=1}^2 (\phi_{ik} - \hat{\phi}_{ik})^2 \quad (7)$$

3 MINIMIZATION OF THE RESIDUAL

The use of numerical methods in conjunction with digital computers has enabled structural engineers to solve a wide variety of complex problems. The CSR, based on observations around or inside the body, involves the determination of the magnitude, extent, and location of the contact stresses acting on Γ . The numerical procedure adopted requires the determination of a model vector $z^T = \{z_1, z_2 \dots z_n\}$ such that $f(z)$ in Eq. (7) be a minimum. Suppose that the location of the contact stress is limited to a bounded set of locations on the boundary $\bar{\Gamma}_1 \subset \Gamma_1$. Constraints, $C_j(z_i) \geq 0$, to prevent contact stress from lying out of the feasible region is adopted. To take $C_j(z_i)$ into account in the minimization process, the internal penalty function (*inverse barrier function*) method is used. Making \mathfrak{R} the penalty parameter, the new augmented objective function is

$$F(z_i, \mathfrak{R}) = f(z_i) + \mathfrak{R} \sum_{j=1}^L \sum_{i=1}^P C_j^{-1}(z_i) \quad (8)$$

There is a lot of methods for the minimization of $F(z_i) = F(z_i, \mathfrak{R})$. The variable metric method is considered to be a powerful optimization method (Reklaitis et al. 1983). In this method, for a fix \mathfrak{R} , $F(z_i)$ is locally approximated, at any point \bar{z} , by a Taylor's expansion

$$F(z) = F(\bar{z}) + \sum_i \frac{\partial F(\bar{z})}{\partial z_i} (z - \bar{z}) + \sum_{i,j} \frac{\partial^2 F(\bar{z})}{\partial z_i \partial z_j} (z - \bar{z})^2 + \dots \quad (9)$$

In matrix notation and including terms up to the 2nd order, Eq. (9) can be rewritten as

$$F(z) \approx A + Bz^T + \frac{1}{2} z^T H z \quad (10)$$

where A is a constant, B is the gradient vector, and the matrix of the second order derivatives, H_z , is the *Hessian* of $F(z_i)$. From Eq. (10), the gradient of the $F(z)$ is $\nabla F(z) = Hz - B$. The variable metric methods iteratively build up a good approximation to H^{-1} . It constructs, during the iterations ($k \rightarrow \infty$), a sequence of matrices $\Lambda^{(k)}$ that will converge to H^{-1} . If the minimum of $F(z_i)$ is achieved in N finite number of iterations, then $\Lambda^{(k)}$ can be used to update z . Suppose z^* gives the minimum of $F(z_i)$, then $\nabla F(z^*) = Hz^* - B = 0$. At any iteration $z^{(k)}$, $H_z^{(k)} = \nabla F(z^{(k)}) - B$. Subtracting this equation from the first one, and multiplying the resultant expression by the matrix H^{-1} , it yields

$$z^* - z^{(k)} = -H^{-1}[\nabla F(z^{(k)})] \quad (11)$$

The left-hand side of Eq. (11) represents a finite step to take the vector $z^{(k)}$ towards the exact minimum z^* . Subtracting Eq. (11) at $z^{(k+1)}$ from the same equation at $z^{(k)}$ gives

$$z^{(k+1)} - z^{(k)} = -H^{-1}[\nabla F(z^{(k+1)}) - \nabla F(z^{(k)})] \quad (12)$$

In the variable metric method, the sequence $\Lambda^{(0)}, \Lambda^{(1)}, \Lambda^{(2)}, \dots, \Lambda^{(k+1)}$ approaches H^{-1} in a finite number of iterations. In this paper, the recursive formulae from the BFGS (Reklaitis et al. 1983) algorithm are applied to update $\Lambda^{(k+1)}$. Knowing that $g^{(k)} = \nabla F(z^{(k)}, \mathfrak{R})$, $\Delta z^{(k)} = z^{(k+1)} - z^{(k)}$, and $\Delta g^{(k)} = g(z^{(k+1)}) - g(z^{(k)})$, $\Lambda^{(k+1)}$ is updated as

$$\Lambda^{(k+1)} = \Lambda^{(k)} - \frac{\Lambda^{(k)} \Delta z^{(k)} \Delta g^{(k)T} \Lambda^{(k)}}{\Delta z^{(k)T} \Lambda^{(k)} \Delta g^{(k)}} + \frac{\Delta g^{(k)} \Delta g^{(k)T}}{\Delta g^{(k)T} \Delta z^{(k)}} \quad (13)$$

Substituting in Eq. (12) H^{-1} for $\Lambda^{(k+1)}$, and calling $s(z^{(k)}) = s^{(k)} = \Lambda^{(k+1)}[\nabla F(z^{(k+1)}) - \nabla F(z^{(k)})]$ then, if we start from an initial guess $z^{(0)}$, the update of $z^{(k)}$ in search of the minimum in the direction of $s^{(k)}$ can be written as

$$z^{(k+1)} = z^{(k)} + \alpha^{(k)} s(z^{(k)}) \quad (14)$$

where $\alpha^{(k)}$ is the step-length along $s^{(k)}$. In the sub-minimization process of finding $\alpha^{(k)}$ to minimize $F(z) = F(z, \mathfrak{R})$, given the initial guess $z^{(0)}$, the derivatives of $F(z^{(0)})$ and the search direction $s^{(0)}$ are calculated. Three values $\alpha^{(a)} < \alpha^{(b)} < \alpha^{(c)}$ corresponding to three points $z^{(a)} < z^{(b)} < z^{(c)}$ in Eq. (14), along the path $s^{(0)}$, are found. These points are such that $F(z^{(a)}) > F(z^{(b)}) < F(z^{(c)})$. To ensure that the location of the vector $z^{(k)}$ lies inside the feasible domain $\bar{\Gamma}_1 \subset \Gamma_1$, the step-length $\alpha^{(k)}$ is successively contracted by 10%, when necessary, until $z^{(k)}$ lies inside the feasible domain. With the three initial points $\alpha^{(a)} < \alpha^{(b)} < \alpha^{(c)}$, Brent's method (Gill et al. 1981) is applied to find the minimum of $F(z)$ along $s^{(0)}$ by approximating the function $F(z)$ by a parabola fitted through $\{\alpha^{(a)}, \alpha^{(b)}, \alpha^{(c)}\}$. With $F^{(a)} = F(z^{(a)})$, $F^{(b)} = F(z^{(b)})$, and $F^{(c)} = F(z^{(c)})$ solving the inverse interpolation problem, the variable $\alpha^{(m)}$ denoting the minimum of the interpolating parabola, is found as

$$\alpha^{(m)} = \alpha^{(b)} + \frac{(\alpha^{(b)} - \alpha^{(a)})^2 [F^{(b)} - F^{(c)}] - (\alpha^{(b)} - \alpha^{(c)})^2 [F^{(b)} - F^{(a)}]}{(\alpha^{(b)} - \alpha^{(a)}) [F^{(b)} - F^{(c)}] - (\alpha^{(b)} - \alpha^{(c)}) [F^{(b)} - F^{(a)}]} \quad (15)$$

Eq. (15) fails if the points are collinear. Brent's method takes care of this situation by shifting to the Golden Section method (Gill et al. 1981). At $\alpha^{(m)}$, $F(z^{(m)})$ is evaluated. $F(z^{(a)})$, $F(z^{(b)})$, and $F(z^{(c)})$ are compared with $F(z^{(m)})$. The one with the most difference is replaced by $F(z^{(m)})$. A new triple set of points is obtained. A parabola is fitted through this new set. The process is applied until the minimum of $F(z)$, along $s^{(k)}$, is found. With $\alpha^{(k)}$, BFGS updates $\Lambda^{(k+1)}$, $s^{(k+1)}$, and $z^{(k+1)}$. If convergence has been achieved the program stops. If not, the next iteration begins with the updated values of $\Lambda^{(k+1)}$, $s^{(k+1)}$, and $z^{(k+1)}$.

4 BEM AND SENSITIVITIES

The most widely used numerical techniques successfully applied to direct problems are the FEM and the BEM. A recent review of the literature indicates that the FEM has been systematically incorporated into numerical schemes for solving IPP (Bezerra 1993). During the last decade, though, the BEM has become an alternative and has emerged as a powerful tool for solving various complex problems. There are many advantages that make the BEM an attractive and competitive technique. BEM has some distinctive advantages, especially for certain classes of linear problems over "domain" type techniques such as the FEM. In the BEM the dimensionality of the problem is reduced. 2D problems are reduced to line integrals. As a "meshless" method the BEM is well suited for problems involving continuous mesh updates. The contact stress reconstruction is an example of such problem. The extent and location of the contact stresses on Γ have to be found and for

that the mesh at the boundary has to be constantly updated. BEM technique makes the mesh update easier. The fundamental equation in the BEM is the Somigliana's identity. Omitting the body force, the Somigliana's identity can be written as

$$u_i = \oint_{\Gamma_1} \bar{u}_{ij}^* t_j + \oint_{\Gamma_2} \bar{u}_{ij}^* t_j - \oint_{\Gamma_1} \bar{t}_{ij}^* u_j - \oint_{\Gamma_2} \bar{t}_{ij}^* u_j \quad (16)$$

$$\text{with } u_i^* = c_1 (c_2 \delta_{ij} \log R - (Y_i Y_j) / R^2) \quad (17)$$

$$t_{ij}^* = (c_3 / R^2) [c_4 (n_k Y_i - n_i Y_k) + (c_4 \delta_{ik} + (2 Y_i Y_k) / R^2) Y_j n_j] \quad (18)$$

where $u_i^* = u_i^*(\xi, x)$, $t_{ij}^* = t_{ij}^*(\xi, x)$, $\mu = E + (2(1 + \nu))$ is the shear modulus, E is the Young's modulus and ν is the Poisson's ratio, $c_1 = -1 + (8\pi\mu(1 - \nu))$, $c_2 = 3 - 4\nu$, $c_3 = -1 + (4\pi(1 - \nu))$, and $c_4 = 1 - 2\nu$. The term $Y_i = x_i + \xi_i$ is the distance between the point load x_i on the boundary and the field point ξ_i , $R^2 = Y_i Y_i$, and n_i are the outward normals at boundary Γ . Similar to Eq. (16), the equation to determine the stresses can be written as

$$\sigma_{ij} = \int_{\Gamma} [e_{ijk}^* t_k - \sigma_{ik}^* u_k] d\Gamma \quad (19)$$

$$\text{with } e_{ijk}^* = e_{ijk}^*(\xi, x) = (a_3 n_l Y_l / R^4) [2 a_2 \delta_{ij} Y_k + 2 \nu (\delta_{ij} Y_k + \delta_{ij} Y_k) - 8 Y_i Y_j Y_k / R^2] + (a_3 / R^2) [n_i (2 \nu Y_j Y_k / R^2 + a_2 \delta_{jk}) + n_j (2 \nu Y_i Y_k / R^2 + a_2 \delta_{ik})] + (a_3 / R^2) [n_k (2 a_2 Y_i Y_j / R^2 - a_4 \delta_{ij})] \quad (20)$$

$$\text{and } \sigma_{ik}^* = \sigma_{ik}^*(\xi, x) = (a_1 / R) [a_2 (\delta_{ik} Y_j + \delta_{ik} Y_j - \delta_{ij} Y_k) / R + 2 Y_i Y_j Y_k / R^3] \quad (21)$$

$a_1 = -c_1$, $a_2 = c_4$, $a_3 = \mu / [2\pi(1 - \nu)]$, $a_4 = 1 - 4\nu$. With the stresses, the strains can be obtained as

$$e_{ij}(\xi) = \sigma_{ij}(\xi) / (2\mu) - 2 \delta_{ij} \sigma_{kk}(\xi) / [2\mu(2\mu + 3\lambda)] \quad (22)$$

For the discretization of Eq.(16), Γ is approximated by piecewise elements. The geometry, displacements, and tractions at Γ_i (a piece of Γ) in discrete coordinates are

$$x_j(\xi) = \sum_{i=1}^3 h^i(\zeta) x_j^{(i)} \quad (23), \quad u_j(\xi) = \sum_{i=1}^3 h^i(\zeta) u_j^{(i)} \quad (24) \quad \text{and} \quad t_j(\xi) = \sum_{i=1}^3 h^i(\zeta) t_j^{(i)} \quad (25)$$

where $x_j^{(i)}$ are the Cartesian coordinates (x, y) defining the geometry; $u_j^{(i)}$ is the nodal displacement; $t_j^{(i)}$ is the nodal traction. $x_j^{(i)}$, $u_j^{(i)}$, and $t_j^{(i)}$ are nodal coordinates, displacements and tractions, respectively, at the nodal point "i." $h_j^{(i)}$ are quadratic interpolating functions in natural coordinate ζ . Putting Eqs. (23), (24), and (25) into Eq. (16) and manipulating the resulting equation with modal $u_j^{(i)} \in \{U\}$ in one side and $t_j^{(i)} \in \{T\}$ on the other side, we get

$$[F]\{U\} = [G]\{T\} \quad (26),$$

$$\text{with } G_{pq} = \sum_{k=1}^{N_e} \int_{-1}^1 [u_{ik}^* h] h_j d\zeta \quad (27), \quad \text{and} \quad F_{pq} = \sum_{k=1}^{N_e} \int_{-1}^1 [t_{ik}^* h] h_j d\zeta \quad (28)$$

where G_{pq} and F_{pq} are the terms of the matrices $[F]$ and $[G]$, respectively. The indices "p" and "q" denote node and element, respectively; N_e is the total number of elements in the mesh. G_{pq} and F_{pq} are the interaction coefficients relating node "q" with all the nodes on the surface of the body. The system of Eq. (26) may be rearranged after all the prescribed boundary conditions (tractions \bar{t} and displacements \bar{u}) are imposed. The manipulation of Eq. (26) is done to transfer all the unknowns to the left-hand side and all the known quantities to the right-hand side, resulting in $[A]\{v\} = \{b\}$. $\{v\}$ is the vector of unknowns and $\{b\}$ the vector of known boundary conditions multiplied by some other matrix resulting from the manipulation operations due to the application of the boundary conditions. Upon finding $\{v\}$, the displacements at any location can be found from Eq. (16). In the same way, applying the boundary values in the discretized form of Eq. (21), the stresses (and the strains by Eq. (22)) can be calculated. Minimizing Eq. (8) by the variable method requires the gradient of $F(z_i) = F(z_i, \mathfrak{R})$ with respect to $z^T = \{z_1, z_2, \dots, z_n\}$.

$$\frac{\partial F(z)}{\partial z} = \frac{\partial F(z, \mathfrak{R})}{\partial z} = 2w \sum_{k=1}^m \sum_{i=1}^2 (\varphi_{ik} - \hat{\varphi}_{ik}) \frac{\partial \varphi_{ik}}{\partial z} - \mathfrak{R} \sum_{j=1}^L \left[\frac{1}{C_j^2(z)} \frac{\partial C_j(z)}{\partial z} \right] \quad (29)$$

The Hessian matrix is approximated by the BFGS algorithm and for that the first-order derivatives of the function $F(z_i)$ in Eq.(29) is needed. In Eq. (29), $\partial \varphi_{ik} / \partial z$ are the sensitivities of displacements, strains, and stresses, depending on what experimental quantities are used in the data vector $\{\hat{\varphi}\}$. To find $\partial \varphi_{ik} / \partial z$ the first derivatives of the boundary displacements and boundary tractions are needed. To accomplish this, the implicit differentiation of Eq. (26) with respect to the design variable, z , leads to

$$[F]_{,z} \{U\} + [F]_{,z} \{U\} = [G]_{,z} \{T\} + [G]_{,z} \{T\} \quad (30)$$

$$\text{with } G_{pq,x} = \sum_{k=1}^{N_x} \int_{-1}^{+1} \{ [u_{ik}^*] h \} J_{k,x} d\zeta \quad (31), \text{ and } F_{pq,x} = \sum_{k=1}^{N_x} \int_{-1}^{+1} \{ [t_{ik}^*] h \} J_{k,x} d\zeta \quad (32)$$

The derivative of the kernels $u_{ij,z}^*$ and $t_{ij,z}^*$ with respect to vector z are, respectively

$$u_{ij,z}^* = u_{ij,z}^*(\xi, x) = c_1 \left[c_2 \delta_{ij,z} / R - (Y_{i,z} Y_j + Y_i Y_{j,z}) / R^2 + 2 Y_i Y_{j,z} / R^3 \right] \quad (33)$$

$$\text{and } t_{ij,z}^* = t_{ij,z}^*(\xi, x) = (c_3 c_4 / R^2) (n_j Y_{i,z} + n_{j,z} Y_i - n_i Y_{j,z} - n_{i,z} Y_j) + (c_3 / R^4) \left[2 Y_i Y_j (Y_{k,z} n_k - Y_{k,n} n_{k,z}) \right. \\ \left. + 2 (Y_{i,z} Y_j + Y_i Y_{j,z}) Y_{k,n} - 8 Y_i Y_j Y_{k,n} R_{,z} / R \right] - (2 c_3 / R^3) \left[c_4 (n_j Y_i - n_i Y_j) - (c_4 \delta_{ik} + (2 Y_i Y_j) / R^2) \right] R_{,z} \quad (34)$$

where $R_{,x} = R^{-1} Y_k Y_{k,x}$, $n_{z,x} = J^{-2} J_{,x} x_{1,x} + J^{-1} x_{1,x}$, and $n_{i,x} = -J^{-2} J_{,x} x_{2,x} + J^{-1} x_{2,x}$.

The singularities in $G_{pq,x}$ and $F_{pq,x}$ were studied by (Saigal et al. 1989). Knowing $\{G\}_{,x}$ and $\{F\}_{,x}$ and manipulating Eq. (30) results $\{F\}(U)_{,z} = \{G\}(T)_{,z} + \{r\}$ with $\{r\} = \{G\}_{,x} \{T\} - \{F\}_{,x} \{U\}$. After applying the sensitivity boundary conditions in that equation one arrives to $\{A\}\{v\}_{,z} = \{d\} + \{r\}$, where $\{v\}_{,z}$ contains both the boundary displacement and boundary traction derivatives. With such derivatives, the displacement, stress, and strain sensitivities at any filed point, can be found through the derivatives of Eqs. (16), (19), and (22), respectively. The derivative of Eq. (16) needs the kernels' sensitivities in Eqs. (33) and (34). The stress sensitivity needs the strain and stress kernel derivatives as follows

$$\epsilon_{ijk,z}^* = \epsilon_{ijk,z}^*(\xi, x) = -4(a_3 n_{i,z} Y_l / R^4) (a_3 n_{l,z} Y_1 / R^4) (a_3 n_{l,z} Y_l R_{,z} / R^5) \left[2 a_2 \delta_{ij} Y_k \right. \\ \left. + 2 \nu (\delta_{ik} Y_j + \delta_{jk} Y_i) - 8 Y_i Y_j Y_k / R^2 \right] + (a_3 n_{l,z} Y_l / R^4) \left[2 a_2 \delta_{ij} Y_{k,z} + 2 \nu (\delta_{ij} Y_{j,z} + \delta_{ij} Y_{k,z}) \right. \\ \left. - (8 / R^2) (Y_{i,z} Y_j Y_k + Y_i Y_{j,z} Y_k + Y_i Y_j Y_{k,z} + 2 R_{,z} Y_i Y_j Y_k / R) \right] - (2 R_{,z} a_3 / R^3) \\ \left[n_i (2 \nu Y_j Y_k / R^2 + a_2 \delta_{jk}) + n_j (2 \nu Y_i Y_k / R^2 + a_2 \delta_{ik}) \right] + (a_3 / R^2) \left[n_{i,z} (2 \nu Y_j Y_k / R^2 + a_2 \delta_{jk}) \right. \\ \left. + (2 \nu n_i / R^2) (Y_{j,z} Y_k + Y_j Y_{k,z} - 2 R_{,z} Y_i Y_k / R) + n_{j,z} (2 \nu Y_j Y_k / R^2 + a_2 \delta_{jk}) + (2 \nu n_j / R^2) \right. \\ \left. (Y_{j,z} Y_k + Y_j Y_{k,z} - 2 R_{,z} Y_i Y_k / R) \right] - (2 a_3 R_{,z} / R^3) \left[n_k (2 a_2 Y_i Y_j / R^2 - a_4 \delta_{ij}) + (a_3 / R^2) \right. \\ \left. \left[n_{k,z} (2 a_2 Y_i Y_j / R^2 - a_4 \delta_{ij}) + (2 a_2 n_k / R^2) (Y_{i,z} Y_j + Y_i Y_{j,z} - 2 R_{,z} Y_i Y_j / R) \right] \right] \quad (35)$$

$$\sigma_{ijk,z}^* = \sigma_{ijk,z}^*(\xi, x) = -(a_1 R_{,z} / R^3) \left[a_2 (\delta_{ik} Y_j + \delta_{jk} Y_i - \delta_{ij} Y_k) + 2 Y_i Y_j Y_k / R^2 \right] + (a_1 / R^2) \\ \left[a_2 R_{,z} (\delta_{ik} Y_j + \delta_{jk} Y_i - \delta_{ij} Y_k) / R + a_2 (\delta_{ik} Y_{j,z} + \delta_{jk} Y_{i,z} - \delta_{ij} Y_{k,z}) / R + 2 Y_i Y_j Y_{k,z} / R^3 \right. \\ \left. + 2 Y_i Y_{j,z} Y_k / R^3 + 2 Y_i Y_j Y_{k,z} / R^3 + 6 R_{,z} Y_i Y_j Y_k / R^3 \right] \quad (36)$$

When strains are the measured quantities in the data vector, the strains sensitivities are needed in the minimization process. Knowing the stress sensitivities, the strain sensitivities can be obtained by deriving Eq.(22) w.r.t. vector z .

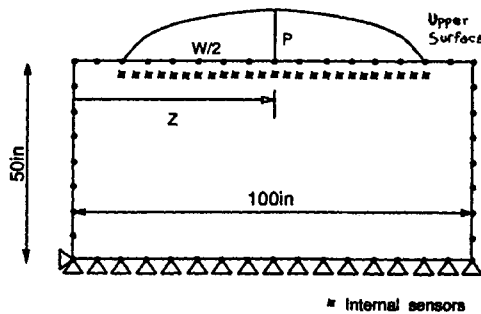


Fig.2: Panel with contact stress

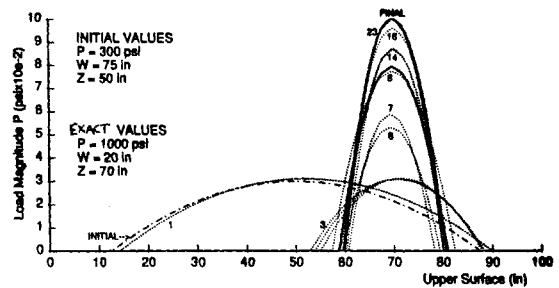


Fig.3: Parabolic contact stress

5 NUMERICAL EXAMPLES

In the examples, the experimental data vector $\hat{\phi}_{ik}$ will be stresses and strains, respectively, for the first and second example. $\hat{\phi}_{ik}$ was obtained from a priori direct BEM analysis with the actual boundary tractions on the structures. These tractions are the "exact" solution for the purposes of comparison of the accuracy of the present procedures.

A panel under parabolic tractions: The panel in Fig. 2 is considered to get in touch with another structure. The panel properties are: $E = 18.6 \times 10^6$ psi, and $\nu = 0.3$. At 39 internal sensors (crosses at Fig. 2) the stresses along "x-y" direction is observed while the panel is under an "unknown" normal contact stress with parabolic distribution at its top edge. The location, Z, the span, W, and the peak magnitude, P, of the contact stress are unknown and desired to be reconstructed. The model vector is $\mathbf{z}^T = \{Z, W, P\}$. The parabolic normal contact stress is $\sigma(s) = (-4P_s^2 + 8PZs + PW^2 - 4PZ^2)/W^2$. "s" is the distance along the span of the parabola and $(Z - 0.5W) \leq s \leq (Z + 0.5W)$. The initial guess for \mathbf{z}^T was $\mathbf{z}^T = \{50\text{in}, 75\text{in}, 300\text{psi}\}$. The evolution of the missing traction distribution is shown in Fig. 3 & 4. The exact traction distribution is shown in bold line in that figure. As the missing contact stress varied in position and span length after each iteration, the mesh for the upper boundary edge was modified to accommodate such evolutions. The parameter η in Eq.(8) was varied during the analysis changing from a value of 10^5 at the beginning to zero at the end. The final solution was obtained in 26 iterations. Table 1 shows the final results obtained with no error in the data vector and also with 5% and 10% random error contaminating the data vector.

A roller under normal and tangential stresses: The contact stresses acting on a roller at its interface with a workpiece are analyzed. The roller is in Fig. 5 and the material has $E = 1217\text{N/mm}^2$ and $\nu = 0.3$. The region coming in contact with the workpiece was discretized with a finer mesh. The measurements were obtained at 25 internal locations identified by solid crosses at Fig. 5. The data vector in this case consists of strains read at 25 internal locations. The contact region is characterized by the angle "γ". The normal traction distribution is assumed to be symmetric and the tangential traction assumed antisymmetric. They are $N(x) = A \sin[\kappa x]$ and $T(x) = B \sin[(\kappa - 0.5)\gamma]$, respectively. A and B are amplitudes of the corresponding traction distribution. Fig. 6 shows the residual function to minimize and the region of the minimum can be identified. The parameters A, B, and γ define the missing traction distributions and constitute the model vector \mathbf{z}^T . Starting with $A = 55\text{N/mm}^2$, $B = 5\text{N/mm}^2$, and $\gamma = 10^\circ$, the normal and tangential contact stress converges to the final solution after 18 iterations and are shown in Fig. 7 and 8, respectively.

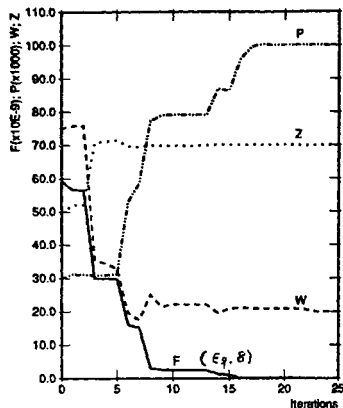


Fig. 4: P, W, & Z convergence

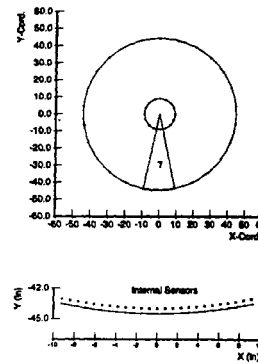


Fig. 5: Roller & sensors locations

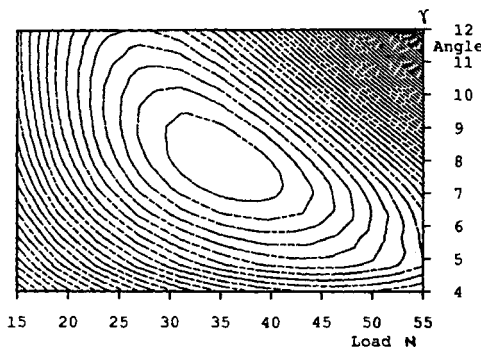


Fig.6 Function contour

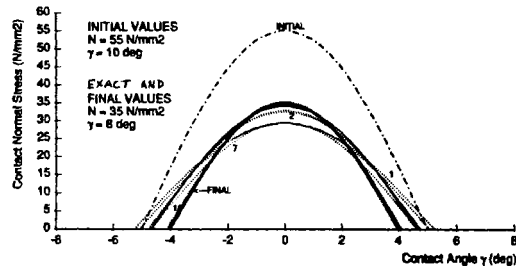


Fig.7 Evolution of normal contact stress

TABLE 1: Panel with Parabolic Contact Stress - Numerical Results: Traction p , Span W , and Position Z

DATA ERROR PARAMETER	STANDARD DEVIATION	P(PSD)	W(IN)	Z(IN)
$\tilde{\eta}=0\%$	$\tilde{\sigma}=0.00$	1000.1	19.99	70.00
$\tilde{\eta}=5\%$	$\tilde{\sigma}_1 = 1.38$ $\tilde{\sigma}_2 = 3.15$	1001.1	19.97	71.11
$\tilde{\eta}=10\%$	$\tilde{\sigma}_1 = 2.76$ $\tilde{\sigma}_2 = 6.31$	1001.8	19.94	71.11

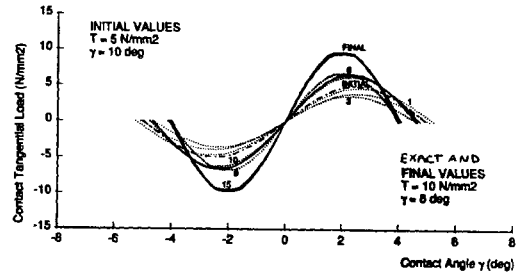


Fig.8: Evolution of tangential contact stress

6 CONCLUSIONS

An optimization-based BEM formulation for the solution of the ill-posed problem of contact stress reconstruction has been presented. The approach to reconstruct contact stress is based on the minimization of the residual between "experimental" data at discrete points and the corresponding computed quantities. To keep the solution in feasible domains, constraint equations are imposed. The *inverse* penalty function was augmented to the objective function so that the constrained problem was transformed into an unconstrained one. The minimization is performed using a quasi-Newton method with implicit differentiation of the kernels of the BEM equations. Parabolic and sinusoidal stress distributions were assumed for the unknown contact stress. The magnitude, extent, and location of the unknown contact stresses were closely predicted demonstrating the validity of the approach to reconstruct stress from "experimental" data. A prime limitation of the approach is that the optimization procedure may converge to a local minimum.

REFERENCES

- Balas, J., J. Sladek, and M. Drzik. 1983. Stress analysis by combination of holographic interferometry and boundary integral methods. *Experimental Mechanics*, 23: 196-202.
- Bezerra L. M. 1993. Inverse Elastostatics Solutions With Boundary Elements. PhD Thesis. Carnegie Mellon University. Pittsburgh, PA.
- Gill P. E., W. Murray, and M. H. Write. 1981. *Practical Optimization*. London: Academic Press.
- Reklaitis G. V., A. Ravindran, and K. M. Ragsdell. 1983. *Engineering Optimization - Methods and Applications*. New York: John Wiley.
- Saigal S., R. Aithal, and J. H. Kane. 1989. Conforming boundary elements in plane elasticity for shape design sensitivity. *Int. J. Num. Methods in Eng.*, 28: 2795-2911.
- Schnur D. S., and N. Zabaras. 1990. Finite element solution of two-dimensional inverse elastic problem using spatial smoothing. *Int. J. for Num. Methods in Eng.*, 30: 57-75.
- Weathers J. M., W. A. Foster, W. F. Swinson, and J. L. Turner. 1985. Integration of laser-speckle and finite element techniques of stress analysis. *Experimental Mechanics*. 25: 60-65.

